

ORIGINAL ARTICLE

Circulating extracellular vesicle-associated TGF β 3 modulates response to cytotoxic therapy in head and neck squamous cell carcinoma

Dorival Mendes Rodrigues-Junior^{1,2}, Soon Sim Tan³, Sai Kiang Lim³, Hui Sun Leong², Matias Eliseo Melendez⁴, Cintia Regina Niederauer Ramos⁴, Luciano de Souza Viana⁴, Daniel S.W.Tan^{2,5}, Andre Lopes Carvalho⁴, N.Gopalakrishna Iyer^{2,6} and Andre Luiz Vettore^{1,*}

¹Department of Biological Sciences, Universidade Federal de São Paulo, Diadema, Brazil, ²Cancer Therapeutics Research Laboratory, National Cancer Centre of Singapore, Singapore, ³Institute of Medical Biology, A*-STAR, Singapore, ⁴Molecular Oncology Research Center, Barretos Cancer Hospital, Barretos, Brazil, ⁵Division of Medical Oncology, National Cancer Centre of Singapore, Singapore and ⁶Division of Surgical Oncology, National Cancer Centre of Singapore, Singapore

*To whom correspondence should be addressed. Laboratório de Biologia Molecular do Câncer, Universidade Federal De São Paulo (UNIFESP), Rua Pedro de Toledo, 669-11° andar, São Paulo, SP 04039-032, Brazil. Tel: +551155764848; Email: andre.vettore@gmail.com
Correspondence may also be addressed to N. Gopalakrishna Iyer. Email: gopaliyer@nccs.com.sg

Abstract

Management of locally advanced head and neck squamous cell carcinoma (HNSCC) requires a multi-prong approach comprising surgery, radiation and/or chemotherapy, yet outcomes are limited. This is largely due to a paucity of biomarkers that can predict response to specific treatment modalities. Here, we evaluated TGF β 3 protein levels in extracellular vesicles (EVs) released by HNSCC cells as a predictor for response to chemoradiation therapy (CRT). To this end, specific EV-fractions were isolated from cell lines or HNSCC patient plasma, and TGF β 3 protein was quantified. In patients treated with CRT, TGF β 3 levels were found to be significantly higher in plasma EV-fractions or non-responders compared with responders. High levels of TGF β 3 levels in Annexin V-EVs were associated with the worst progression-free survival. *In vitro* experiments demonstrated that TGF β 3 silencing sensitized HNSCC cells to cytotoxic therapies, and this phenotype could be rescued by treatment with exogenous. In addition, specific EV-fractions shed by cisplatin-resistant cells were sufficient to transfer the resistant phenotype to sensitive cells through activation of TGF β -signaling pathway. Therefore, our data show that TGF β 3 transmitted through EV plays a significant role in response to cytotoxic therapy, which can be exploited as a potential biomarker for CRT response in HNSCC patients treated with curative intent.

Introduction

Biomarker-directed therapeutic decisions remain the cornerstone for precision oncology, most widely practiced in the utilization of targeted therapy. However, it is equally critical to define biomarkers of response to conventional cytotoxic therapy, commonly used for most solid tumors. This is evident in head and neck squamous cell carcinoma (HNSCC), which is one of the most common lethal malignancies worldwide (1,2).

For locally advanced HNSCC affecting the oropharynx, larynx and hypopharynx, concurrent chemoradiation therapy (CRT), with or without induction chemotherapy (IC) has been established as the paradigm of treatment with curative intent (3). Nonetheless, a significant number of patients fail to respond and develop recurrent/progressive disease, where surgery is the only available option. For these patients, ineffective treatment

Abbreviations

AV	Annexin V
CisR	cisplatin resistant
CTB	<i>Cholerae</i> Toxin chain B
CR	complete response
CRT	chemoradiation therapy
ELISA	enzyme-linked immunosorbent assay
EV	extracellular vesicle
HNSCC	head and neck squamous cell carcinoma
IC	induction chemotherapy
PBS	phosphate-buffered saline
PR	partial response
RT-qPCR	reverse transcription quantitative polymerase chain reaction
TGFβ	transforming growth factor beta
WT	wild type
VSF	vesicular secretome fraction

choices result in an unwanted delay of potentially curative surgery. In addition, surgery is made challenging in a heavily pretreated patient and a radiated field (4). The ability to predict treatment failure and identify patients early could help to optimize treatment decisions and direct patients to more aggressive treatment up-front. Therefore, there is an unmet need for robust and ideally non-invasive predictive biomarkers for HNSCC treated with CRT.

In this context, non-invasive, robust blood-based markers are ideal, and if these can be shown to be involved in the biology of treatment response also have the additional potential to be therapeutic targets (5). However, identifying putative markers in the blood, plasma or serum is fraught with many technical issues, especially the presence of high-abundance proteins in these compartments, resulting in low signal-to-noise ratio. The discovery of extracellular vesicles (EVs: exosomes, microvesicles, apoptotic bodies) could circumvent these issues and allow analyses of a much 'cleaner' serum/plasma compartments (6).

EVs are lipid bilayer membrane vesicles carrying proteins, lipids, nucleic acids and sugars (6,7). Tumor cells are avid EV producers, which can function in a paracrine manner or carried through the circulation to target cells (8,9), where their cargo can influence immune evasion, tumorigenesis, cancer progression, metastatic spread and response to treatment (10–12). Of note, HNSCC are known to produce EVs into the circulation (13,14). These could potentially be used in diagnosis, prognosis and predicting response to treatment, as they offer a non-invasive window into the tumor and its microenvironment (15). In particular, EVs have been implicated in mediating drug resistance in tumor cells by transferring proteins such as P-glycoprotein (ABCB1) able to export drugs or sequester drugs in EVs for removal from tumor cells or transferring micro RNA to activate genes to counter the effects of the drugs in recipient cells (11).

We recently conducted a high-throughput screen of specific plasma EVs, comparing responders and non-responders in HNSCC treated with CRT to identify potential markers of treatment response (16). Among the potential markers in plasma EVs, TGFβ3 emerged as a putative candidate that correlated with treatment. Previous studies have shown that transforming growth factor beta (TGFβ) signaling appears to have a widespread function in tumor initiation, progression and metastases (17–19). TGFβ superfamily has also been implicated in epithelial-mesenchymal transition and in maintaining the stem cell fraction, which in turn plays an important role in radio- and chemoresistance. Consistent with this, TGFβ1 expression in

HNSCCs has been shown to correlate with poor disease outcome, but not with treatment response (20,21). Although plasma levels of TGFβ have been used as a prognostic marker in gastric, breast, lung, hepatocellular, colorectal and renal cell carcinomas (22–27), its use in HNSCC, especially in the context of treatment response remains untested.

On the basis of our previous screen, we, therefore, examined the association of circulating EV-associated TGFβ3 with resistance to cytotoxic chemo- and radiation therapy in HNSCC. Our data demonstrate the potential of TGFβ3 in circulating EVs as a potential blood-based predictive biomarker for treatment response in HNSCC patients treated with CRT and suggests a role for EV-TGFβ3 signaling in mediating resistance to cytotoxic drugs.

Material and methods**Patients and trial**

This study involved plasma samples from 38 patients with locally advanced HNSCC who underwent chemoradiotherapy protocol as part of a phase 2 clinical trial to test the effect of IC followed by concomitant CRT in the treatment of HNSCC patients between 2009 and 2010 at the Department of Head and Neck Surgery, Barretos Cancer Hospital (Barretos, São Paulo, Brazil). In summary, IC consisted of intravenous paclitaxel (175 mg/m²) and cisplatin (80 mg/m²), and CRT consisted of concomitant radiotherapy (2 Gy/day, 5 days/week for 7 weeks) and cisplatin (100 mg/m², administered intravenously on days 1, 22 and 43), initiated at 3 weeks after the third cycle of IC (4).

This study was approved by the ethics committees of Federal University of São Paulo (#1610/2016) and Barretos Cancer Hospital (#231/2009). The study included patients with histologically confirmed locally advanced stage III or IV a-b (M0) squamous cell carcinoma of the oral cavity, larynx, oropharynx, or hypopharynx, that signed an informed consent to undergo the treatment as outlined. All patients were required to have measurable disease by Response Evaluation Criteria in Solid Tumors (RECIST, version 1.1) at the start point, and disease response was evaluated after IC and after CRT using the RECIST criteria. Briefly, tumor response to treatment was considered as complete response (CR) when there was the disappearance of all detectable lesions, and non-response (NR) as tumor response less than complete, the appearance of a new lesion, or increase of any lesion classified as measurable at initial examination (including tumor recurrence). Further details of the trial, including the definition of tumor response as partial response (PR), stable disease) or progression of disease can be found in the previously published results (4). For statistical analysis, patients with CR and PR after IC were grouped and compared with those with stable disease or progression of disease. On the other hand, when considering CRT response, only patients with CR were compared with all NR patients, which included those presenting PR, stable disease or progression of disease after the completion of the treatment protocol. All plasma samples were collected at diagnosis, before CRT (pretreatment samples).

Cell line culture and treatment

HNSCC cell lines used in this study were either obtained from ATCC (FaDu-ATCC HTB-43 and SCC25-ATCC CRL-1628) or patient-derived (NCC-HN120 and NCC-HN137). The cisplatin-resistant (CisR) lines used in this study were previously described (28,29). The authenticity of the commercial cell lines was confirmed by short tandem repeat profiling method, which was carried out 6 months before the start of the experiments. For drug treatment, control cells (CTRL) were treated with 10 μM TGFβR inhibitor (TGFβRi; #LY2109761, Cayman Chemical, MI) and the cells-TGFβ3 with 10 ng/ml of exogenous TGFβ3 (#PT-4124; Lonza, Basel, Switzerland). Subsequent cytotoxic drug doses were as follows for SCC25 and FaDu cells: 5.0 μM and 10 μM of cisplatin (#PHR1624; Sigma-Aldrich, St Louis, MO) or 0.01 μM and 0.03 μM of paclitaxel (#PHR1803; Sigma-Aldrich), respectively. Proliferation was quantified using MTS assays (CellTiter-Glo; Promega, Madison, WI) according to the manufacturer's protocol. The relative luminescence units from treated wells were normalized against dimethyl sulfoxide control

wells and expressed as a percentage of viable cells. Apoptosis was quantified using Annexin V-FITC assays according to the manufacturer's protocol (#1006; Biovision, San Francisco, CA). All treatment experiments were performed in triplicate, with three separate biological replicates for each assay.

For cell lines EVs-based treatment, cisplatin-sensitive cells were incubated for 72 h with cisplatin (1.0 μM) or paclitaxel (0.01 nM) in EV-free media, which consists of RPMI-1640 (ThermoFisher, Waltham, MA) supplemented with 10% fetal bovine serum (ThermoFisher) and 0.01 $\mu\text{g/ml}$ penicillin-streptomycin (ThermoFisher) filtered in a 50 kDa Ultra-15 Centrifugal Filter (Amicon, Millipore, MA), with or without the addition of the vesicular secretome fraction (VSF; volume normalized to the equivalent to 100 ng CD81) previously harvested from CisR cells. After this co-treatment, functional assays were performed to observe if EVs could mediate cisplatin response.

EVs isolation

To isolate EVs, the cells were incubated for 72 h in phenol-red free-DMEM (#31053; Gibco, Waltham, MA), supplemented with 5% Insulin-Transferrin-Selenium-Ethanolamine (#51500-056; ThermoFisher), 10 mM Non-Essential Amino Acids (#11140-050; ThermoFisher), 500 μg fibroblast growth factor-basic (#13256-029; ThermoFisher), 100 mM of Sodium Pyruvate and 55 mM of β -Mercaptoethanol (#21985-023; ThermoFisher). After 72 h, the culture medium was collected and centrifuged at 250g for 5 min to remove the dead cells. The supernatant was filtered on a 0.22 μm filter and further concentrated 20 \times by tangential flow filtration on a 50 kDa Ultra-15 Centrifugal Filter (Amicon) by centrifugation at 1200g for 20 min. This concentrated fraction is the VSF.

EVs fractions could be differentiated by their membrane phospholipid composition: specifically GM1-gangliosides and phosphatidylserine, which have a high specific binding affinity for *Cholerae* Toxin chain B (CTB) and Annexin V (AV), respectively (30,31). Briefly, 150 μl plasma or 100 μl VSF was incubated with 0.5 μg biotinylated CTB (#C34779; ThermoFisher) or 0.5 μg biotinylated AV (#K109; Biovision, San Francisco, CA) in 100 μl phosphate-buffered saline (PBS) or AV binding buffer, respectively for 60 min at 37°C. After the addition of 50 μl pre-washed Dynabeads MyOne Streptavidin T1 (#65602; ThermoFisher), the mixture was incubated for 30 min at 25°C. The magnetic beads were immobilized and the supernatant was collected as EV-depleted fraction. The beads were washed three times with 200 μl PBS, and the isolated EVs bound to CTB or AV-beads were stored at -20°C for up to 30 days.

Characterization of EVs

The size distribution of EVs present in the VSF was measured using the ZetaView (Particle Metrix, Ammersee, Germany) or NanoSight (Malvern, Worcestershire, UK). The modal diameter of the EVs was used in the statistical analyses. To visualize EVs through scanning electron microscopy, the VSF preparation was incubated with biotinylated CTB or AV, and CTB-/AV-bound EVs were captured on streptavidin-coated polystyrene particles (#SVP-15-5; Spherotech, Chicago, IL), as previously described (31). The beads were suspended in 50 μl PBS and fixed with formaldehyde solution (formaldehyde 2%, glutaraldehyde 2.5%, sodium cacodylate 0.1 M pH 7.2) before scanning on a FEI Quanta 250 FEG scanning electron microscope (ThermoFisher).

Enzyme-linked immunosorbent assay

Enzyme-linked immunosorbent assay (ELISA) was used to quantify CD81 and TGF β 3 in CTB- or AV-EV fraction present in VSF or plasma samples. For CD81 detection, after EVs extraction, immobilized beads were washed twice with 100 μl wash buffer (0.1% BSA in PBS) and incubated with 100 μl 1:500 diluted anti-CD81 antibodies (#SC-7637; Santa Cruz Biotechnologies, Dallas, TX), washed and incubated again with 1:5000 diluted HRP-conjugated goat anti-mouse secondary antibodies 1:5000 diluted (#SC-2031; Santa Cruz Biotechnologies). HRP activity was determined using Amplex Red Substrate (Life Technology, Grand Island, NY) as per manufacturer's protocol. The relative levels of CD81 in CTB- or AV-EVs were established as the ratio of the number of total cells (x) per total protein amount that was measured when the VSF was collected (y), by the respective concentration of CD81 (z) [(x/y)/z]. For TGF β 3 uncovering, CTB- and

AV-EVs isolated were lysed with cell lysis buffer (#K269; Biovision), and ELISA sandwich assay was conducted following the manufacturer's instructions (#LS-F2825; LSBio, Seattle, Washington, DC), in which the EVs content and crude plasma were previously incubated with solution A (1 N HCl) and B (1.2 N NaOH/0.5 M HEPES) for TGF β 3 activation. The CD81 expression level normalized the relative expression level of TGF β 3 (pg/ml) in EVs shed by cell lines.

RNA extraction, cDNA synthesis and RT-qPCR

RNA extraction and reverse transcription quantitative polymerase chain reaction (RT-qPCR) were performed as previously described (32). Expression levels of the three isoforms of TGF β were determined by RT-qPCR using *beta-actin* (ACTB) levels to normalize expression. The primer sequences for TGF β isoforms were previously described (33).

Knockout—CRISPR-Cas9 system

pSpCas9(BB)-2A-Puro (pX459) V2.0 plasmid was used as a delivery system (34). gRNA sequences targeting TGF β 3 and a scramble gRNA (Supplementary Table 1, available at *Carcinogenesis* Online) were cloned at BbsI restriction site of pX459 plasmid. After sequencing validation, transfections were performed by electroporation using a Nucleofector 2b following the manufacturer's recommendations (Cell Line Nucleofector Kit C, program X-005; Lonza, Basel, Switzerland) with 2.0 μg pX459-gRNA plasmids and 1×10^6 cells. Cells transfected with scramble CTRL and cells ^{-TGF β 3} (TGF β 3 knocked-out) were selected with puromycin (FaDu 2.5 μM and SCC25 1.0 μM). The TGF β 3 knockout was confirmed by western blot (WB).

Western blot

WBs were performed as previously described (29). Antibodies used were purchased from Cell Signaling [MA; anti-SMAD2 (#5339), anti-pSMAD2 (#18338), anti-ERK (#4695), anti-pERK (#4370), anti- α -TUBULIN (#2148), anti-GAPDH (#8884), goat anti-mouse (#7076), anti-rabbit IgG HRP-linked (#7074)] or from Santa Cruz Biotechnology [Dallas, TX; anti-TGF β 3 (#166833), anti-CD9 (#SC-13118) and anti-CD81 (#SC-7637)]. ImageJ bundled with Java 1.8.0_172 (US National Institutes of Health, MD) was used to normalize TGF β 3 intensity, according to α -TUBULIN expression.

Statistical analyses

Comparison of values obtained in cell viability and cell death assays were analyzed with GraphPad Prism 6 (GraphPad Software, San Diego, CA) using one-way ANOVA, and multiple paired comparisons were conducted by means of the Bonferroni's post-test method.

Mann-Whitney, χ^2 or Fisher exact tests were used to evaluate the associations between TGF β 3 expression, treatment response, disease progression and clinical variables, as appropriate. The Kaplan-Meier method was used to estimate the progression-free survival of patients, and the log-rank test was used to examine the differences between groups. A multivariate logistic regression was performed to identify the independent variables associated with treatment response in the organ preservation protocol and performed in a step-forward fashion to estimate the odds ratio. The multivariate logistic regression model included clinical and molecular variables with P value <0.20 in the univariate analysis to build a final model. The final model was further adjusted for clinically relevant variables. These statistical analyses were performed using SPSS statistics 23.0 (IBM, NY). A P-value <0.05 was necessary to determine all statistically significant differences.

Results

Plasma TGF β 3 expression correlates with disease progression

We had previously identified TGF β 3 as a potential marker for response to CRT in a high-throughput screen designed to compare plasma EV fractions between responders and non-responders to CRT. To validate these findings, we set out to quantify TGF β 3 protein levels in three distinct plasma compartments of patients treated with CRT: crude plasma, CTB-EVs and AV-EVs.

The clinical and histological features of the 38 patients with locally advanced HNSCC enrolled in this study are presented in [Supplementary Table 2](#), available at *Carcinogenesis* Online. In summary, the median follow-up for this cohort was 4 years and the patients were predominantly males ($n = 34$; 89.5%), with age ranging from 37 to 76 years (median: 56 years). The use of tobacco (current and former) was reported by 36 patients (94.8%), whereas only 5.3% of the cases were human papillomavirus-associated cancers. Primary tumor sites included oral cavity ($n = 2$, 5.3%), oropharynx ($n = 22$, 57.9%), hypopharynx ($n = 5$, 13.2%) and larynx ($n = 9$, 23.7%). Majority of tumors were locally advanced (T3/T4, 92.1%), and during the follow-up period 27 patients (71.1%) demonstrated CR or PR to IC, and 22 patients (57.9%) presented CR to CRT (there were 3 patients who did not complete the treatment protocol, and thus were not evaluated after the CRT).

TGF β 3 concentration was measured in CTB-EVs, AV-EVs and in crude plasma samples from blood obtained from patients prior to any treatment, and quantified using ELISA. TGF β 3 levels in CTB-EVs and AV-EVs had mean and median concentrations of 580.0 and 562.7 pg/ml (range: 73.1–1328 pg/ml), and 666.6 and 672.3 pg/ml (range: 89.9–1390 pg/ml), respectively. In the total plasma samples, TGF β 3 concentration was significantly lower with mean and median of 13.9 and 5.6 pg/ml (range: 0–73.7 pg/ml). Importantly, TGF β 3 concentrations were significantly higher in CTB-EV and AV-EV fractions from non-responders compared with complete responders for both IC and CRT treatments ([Figure 1A](#) and [B](#)). In contrast, crude plasma concentration of TGF β 3 was not associated with treatment response. On the basis of the Youden index obtained from receiver operating characteristic curves for IC response, cutoff values for TGF β 3 concentration in AV-EVs and CTB-EVs were 769.0 pg/ml (area under the receiver operating characteristic curve: 0.912) and 585.0 pg/ml (area under the receiver operating characteristic curve: 0.838), respectively ([Supplementary Figure 1](#), available at *Carcinogenesis* Online). These cutoff values were used to categorize patients

and determine associations with clinical-pathological characteristics including age, gender, tobacco consumption, primary tumor site, human papillomavirus-status, resectability status, stage and final response to CRT. Statistical analysis shows TGF β 3 concentration in AV-EVs was significantly associated with CRT response ([Table 1](#)). No other associations were observed between the other clinical features and concentration of TGF β 3. In line with this, Kaplan–Meier analysis for progression-free survival showed that patients with higher TGF β 3 levels in AV-EVs had poorer outcomes ([Figure 1C](#)). On the basis of the cutoff defined earlier, 73.3% of patients with high TGF β 3 levels in AV-EVs developed disease progression in 4 years, compared with 52.2% of patients with low TGF β 3 levels ($P = 0.038$). Furthermore, logistic regression analysis adjusted by age, tumor resectability and TGF β 3 levels in plasma AV-EVs showed that TGF β 3 concentration (odds ratio = 9.14; 95% confidence interval = 1.50–55.50; $P = 0.016$) and tumor resectability (odds ratio = 8.67; 95% confidence interval = 1.34–54.84; $P = 0.021$) remained independent prognostic factors for final response to CRT ([Table 2](#)).

TGF β 3 expression in HNSCC cell lines

IC₅₀ levels for cisplatin were determined in two intrinsically resistant lines and in two pairs of isogenic patient-derived lines, where cisplatin resistance was established by stepwise increments of sublethal cisplatin doses. IC₅₀ levels for CisR lines were 36.3 μ M for NCC-HN120 CisR, 13.8 μ M for FaDu, 10.0 μ M for NCC-HN137 CisR and 6.8 μ M for SCC25, whereas IC₅₀ levels for sensitive lines were 2.8 μ M for NCC-HN120 and 1.0 μ M for NCC-HN137 ([Figure 2A](#) and [Supplementary Figure 2](#), available at *Carcinogenesis* Online). RT-qPCR assay was then performed to determine if the expression levels of TGF β correlate with cisplatin sensitivity in these cell lines. We were not able to detect any correlation between cisplatin sensitivity and expression levels of TGF β 1 or TGF β 2 isoforms ([Figure 2B](#) and [C](#)). However, the TGF β 3 expression levels were higher in all four CisR cell lines compared with sensitive lines ([Figure 2D](#)).

Table 1. Correlation between TGF β 3 concentration in AV-EVs and CTB-EVs with clinical and pathological features

Variable	Categories	Number of cases	TGF β 3 in AV-EVs		P (2-tailed)	TGF β 3 in CTB-EVs		P (2-tailed)
			Low n (%)	High n (%)		Low n (%)	High n (%)	
Age (years)	≤60	27	16 (59.3)	11 (40.7)	1.00	15 (55.6)	12 (44.4)	1.00
	>60	11	7 (63.6)	4 (36.4)		6 (54.5)	5 (45.5)	
Gender	Male	34	20 (58.8)	14 (41.2)	1.00	19 (55.9)	15 (44.1)	1.00
	Female	4	3 (75.0)	1 (25.0)		2 (50.0)	2 (50.0)	
Tobacco consumption	Never	2	1 (50.0)	1 (50.0)	0.948	0 (0.0)	2 (100.0)	0.235
	Former	8	5 (62.5)	3 (37.5)		4 (50.0)	4 (50.0)	
	Current	28	17 (60.7)	11 (39.3)		17 (60.7)	11 (39.3)	
Primary site	Oral cavity	2	0 (0.0)	2 (100.0)	0.080	0 (0.0)	2 (100.0)	0.080
	Oropharynx	22	13 (59.1)	9 (40.9)		11 (50.0)	11 (50.0)	
	Hypopharynx	5	5 (100.0)	0 (0.0)		5 (100.0)	0 (0.0)	
	Larynx	9	5 (55.6)	4 (44.4)		5 (55.6)	4 (44.4)	
Human papillomavirus status	Positive (p16+)	2	2 (100.0)	0 (0.0)	0.519	2 (100.0)	0 (0.0)	0.496
	Negative (p16-)	33	20 (60.6)	13 (39.4)		18 (54.5)	15 (45.5)	
Resectability status	Resectable	24	16 (66.7)	8 (33.3)	0.492	15 (62.5)	9 (37.5)	0.318
	Unresectable	14	7 (50.0)	7 (50.0)		6 (42.9)	8 (57.1)	
Stage	III	12	7 (58.3)	5 (41.7)	1.00	6 (50.0)	6 (50.0)	0.734
	IV	26	16 (61.5)	10 (38.5)		15 (57.7)	11 (42.3)	
CRT response	CR	22	17 (77.3)	5 (22.7)	0.012	15 (68.2)	7 (31.8)	0.157
	NR	13	4 (30.8)	9 (69.2)		5 (38.5)	8 (61.5)	

All P values were based on two-tailed t-tests. NR, non-response patients.

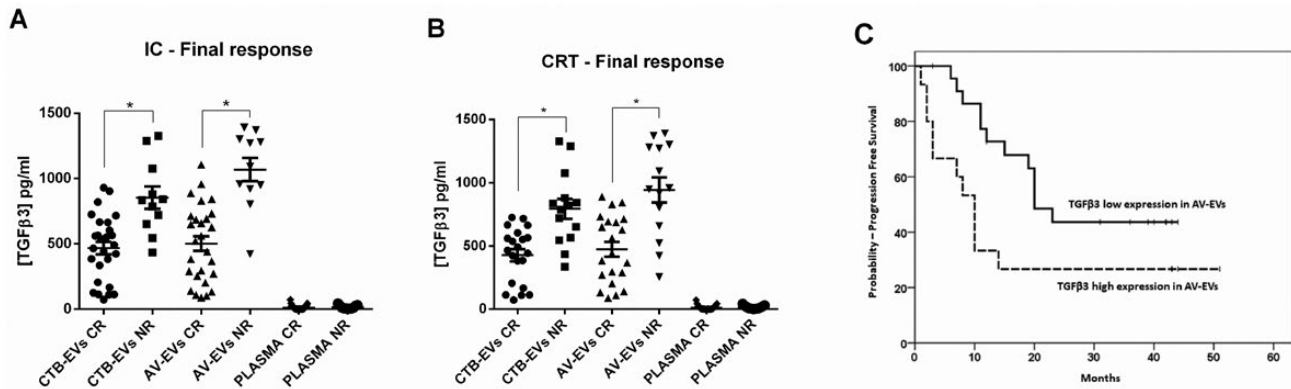


Figure 1. TGF β 3 in plasma-circulating EVs is a prognostic marker for HNSCC CRT. TGF β 3 concentration was measured through ELISA-sandwich (LS-Bio) in EVs present in the plasma of HNSCC patients grouped according to their IC response (A) or CRT final response (B) (* $P < 0.0001$). (C) HNSCC patients' progression-free survival in 4 years according to TGF β 3 concentration in AV-EVs ($P = 0.038$). CRT, chemoradiation therapy; IC, induction chemotherapy; TGF β , transforming growth factor beta.

Table 2. Logistic regression analysis for factors predicting final CRT response

Characteristic	Adjusted OR (95% CI)	P-value
TGF β 3 expression in AV-EVs		
Low expression	1 (ref.)	0.016
High expression	9.14 (1.50–55.50)	
Tumor resectability		
Resectable	1 (ref.)	0.021
Unresectable	8.67 (1.34–54.84)	

CI, confidence interval; OR, odds ratio.

The bold value indicated the statistical significant differences $P < 0.05$.

TGF β 3 knockout sensitizes HNSCC cells to cytotoxic therapy

The CRISPR-Cas9 system was used to knockout TGF β 3 expression in FaDu and SCC25 cell lines to generate SCC25^{-TGF β 3} and FaDu^{-TGF β 3} cells. Compared with parental cells [FaDu wild type (WT) and SCC25 WT] and knockout-scramble control lines (SCC25 CTRL and FaDu CTRL), both knockout cell lines showed dramatic reduction in TGF β 3 expression (reduced by 89.2% for SCC25^{-TGF β 3} and 95.7% for FaDu^{-TGF β 3}; **Figure 3A**). These were subject to drug treatment with either cisplatin or paclitaxel alone, or in the presence of exogenous TGF β 3 in the knockout cells or TGF β receptor II-inhibitor (TGF β Ri) in the CTRL cells. As predicted, SCC25^{-TGF β 3} and FaDu^{-TGF β 3} showed increased drug sensitivity, which was reversed by treatment with exogenous TGF β 3 (**Figure 3B** and **C**). In contrast, abrogating TGF β Ri using the TGF β Ri increased sensitivity to both cytotoxic drugs in SCC25 and FaDu CTRL cells. Similar results were observed when drug effect was evaluated by measuring apoptosis using AV staining assays (**Figure 3D** and **E**). These results support the clinical observation that manipulating TGF β 3 levels is necessary and sufficient to modulate the HNSCC response to cytotoxic therapies.

Secretion and intercellular transfer of TGF β 3-containing EVs by CisR cells

To determine whether HNSCC cell lines secrete TGF β 3 in EVs, culture media conditioned by NCC-HN120 WT and NCC-HN120 CisR were enriched for EVs by filtration. The enriched VSF was analyzed by ZetaView for the presence of nanoparticles. Both WT and CisR VSFs were enriched in nanoparticles with a mean size of 127.1 ± 1.51 nm for WT and 125.9 ± 1.21 nm for CisR (**Supplementary Figure 3A**, available at *Carcinogenesis* Online).

The VSFs were analyzed for the presence of lipid membrane entities by determining if some of the nanoparticles could be extracted by membrane lipid ligands such as CTB or AV. Briefly, the VSF from NCC-HN120 WT were incubated with biotinylated CTB or AV and then with streptavidin-conjugated polystyrene or magnetic beads to immobilize any CTB-EV or AV-EV. The beads were then visualized by scanning electron microscopy and were observed to bind vesicles-like nanoparticles of 100–200 nm consistent with the size range of lipid membrane nanoparticles estimated by ZetaView (**Supplementary Figure 3B**, available at *Carcinogenesis* Online). To further confirm that these lipid membrane nanoparticles were EVs, we assayed CTB- and AV-EVs for the presence of CD81, a tetraspanin membrane protein commonly associated with EVs, by ELISA (**Supplementary Figure 3C**, available at *Carcinogenesis* Online). CD81 was present on both CTB- and AV-EVs secreted by WT and CisR cell lines. Furthermore, the VSF collected from SCC25^{-TGF β 3} was analyzed by NanoSight, and the size distribution of the nanoparticles detected had a mean size of 96.46 ± 5.70 nm (**Supplementary Figure 4A**, available at *Carcinogenesis* Online). The CD9 and CD81 expression was also observed SCC25^{-TGF β 3} by WB (**Supplementary Figure 4B**, available at *Carcinogenesis* Online). Together, these observations confirmed that the VSFs have bona fide 50–200 nm EVs i.e. nano-size particles with membrane lipids, and membrane proteins i.e. EVs.

Next, CTB- and AV-EVs were analyzed for the presence of TGF β 3 by the same ELISA assay used in plasma samples earlier. TGF β 3 protein levels were significantly higher in both CTB- and AV-EV fractions secreted by NCC-HN120 CisR cells compared with those by cisplatin-sensitive NCC-HN120 WT cells (**Figure 4A** and **B**). To determine if EVs could mediate the transfer of the drug-resistant phenotype, VSF from the NCC-HN120 CisR was added to NCC-HN120 WT cultures in the presence of cisplatin or paclitaxel. As predicted, NCC-HN120 WT cells treated with VSF collected from NCC-HN120 CisR cultures became more resistant to cytotoxic drug treatments, indicating that EVs containing high levels of TGF β 3 was sufficient to transfer the resistant phenotype. To further confirm that this effect was EV-mediated, sensitive cells were treated with the same NCC-HN120 CisR-VSF depleted of CTB- or AV-EVs. Drug response assays confirmed that EV depletion could abrogate the resistance-transfer phenotype compared with intact/non-depleted NCC-HN120 CisR VSF. Similarly, VSF collected from SCC25^{-TGF β 3} was unable to induce resistance to cisplatin and paclitaxel in NCC-HN120 WT (**Figure 4C**). VSF-induced drug resistance was associated with increased

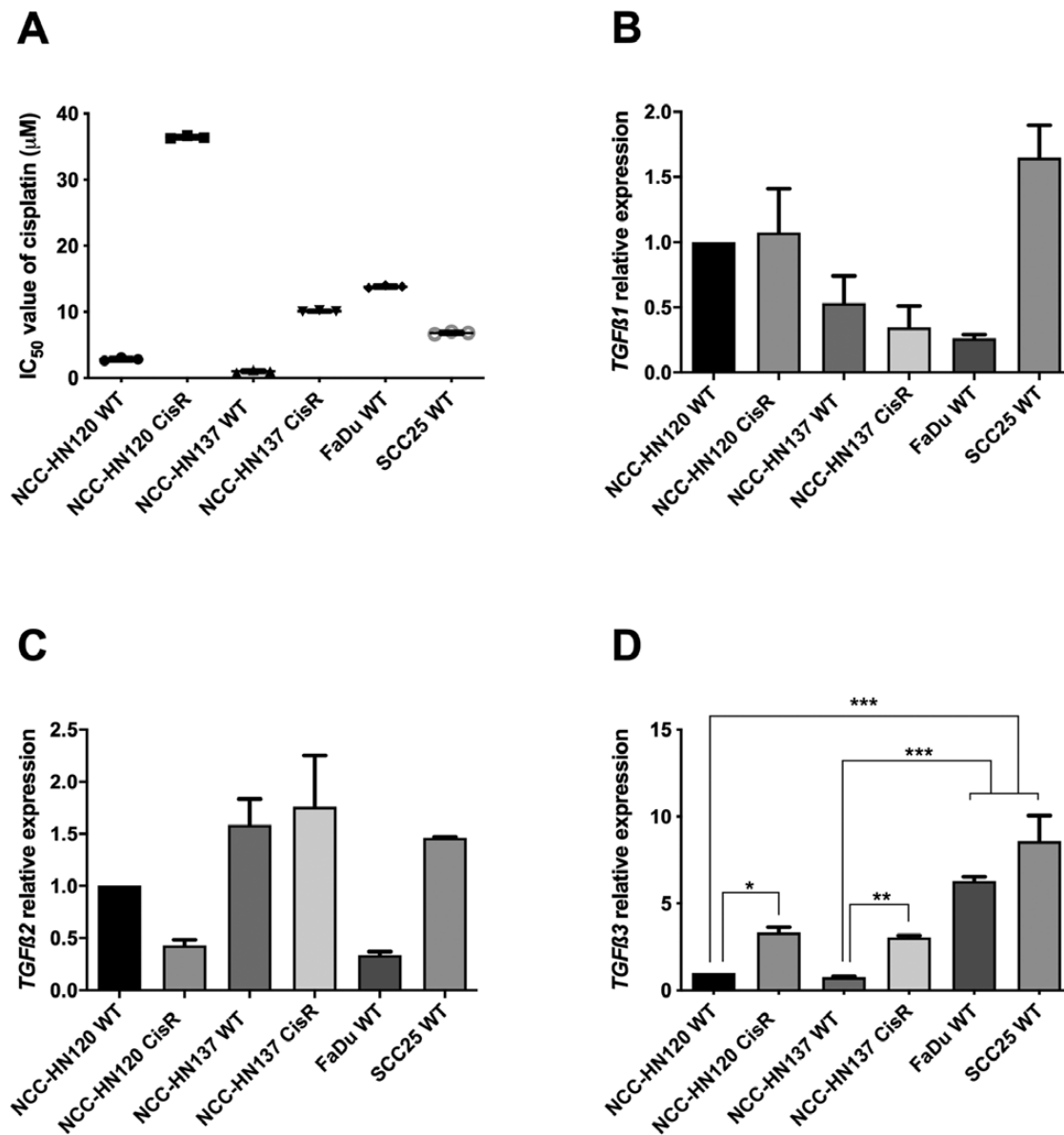


Figure 2. HNSCC cell lines response to cisplatin treatment and expression of $TGF\beta$ isoforms. (A) Assessment of IC_{50} values for cisplatin treatment in NCC-HN120 WT and CisR, NCC-HN137 WT, and CisR, FaDu, and SCC25 cell lines. RT-qPCR analysis was used to evaluate the relative expression level of $TGF\beta 1$ (B), $TGF\beta 2$ (C) and $TGF\beta 3$ (D). All the relative expression levels were calculated using the $2^{-\Delta\Delta Ct}$ method. For all bar graphs, P-values denoted as * $P < 0.05$, ** $P < 0.01$ and *** $P < 0.0001$. IC, induction chemotherapy; TGF β , transforming growth factor beta.

SMAD2 phosphorylation with no effect on ERK phosphorylation, suggesting that the transfer of a resistance phenotype is associated with TGF β downstream signaling (Figure 4D). Taken together, these results suggest that TGF $\beta 3$ present in EVs released by drug-resistant cells are able to activate SMAD2 phosphorylation to induce resistance in sensitive cells.

Discussion

The clinical scenario in this study is not uncommon and remains an unmet need. The ability to predict treatment failures to CRT would redirect HNSCC patients to appropriate curative therapies without delay. In fact, several groups have made attempts to identify factors that predict treatment response based on biological hypotheses and analyses of the primary tumor tissue itself. These include using fresh or archived tissue, and

techniques such as micro RNA expression, single protein biomarkers, complex multi-gene expression or multi-protein signatures (35–37). Extending these to crude plasma-based assays has met with little success to date.

The detection of circulating EVs could circumvent many challenges associated with plasma biomarker discovery. Circulating EV-based biomarkers is an emerging research area with great potential clinical relevance. Shao *et al.* (38) showed that the typing of proteins present in circulating microvesicles allows real-time monitoring of glioblastoma therapy response. One of the major technical issues in many such analyses is the reliability and reproducibility of capture techniques to isolate biologically relevant EVs, particularly the need to move beyond simple centrifugation-based isolation. We had previously shown that it is possible to isolate at least two distinct fractions of EVs in plasma according to CTB or AV ligands, which

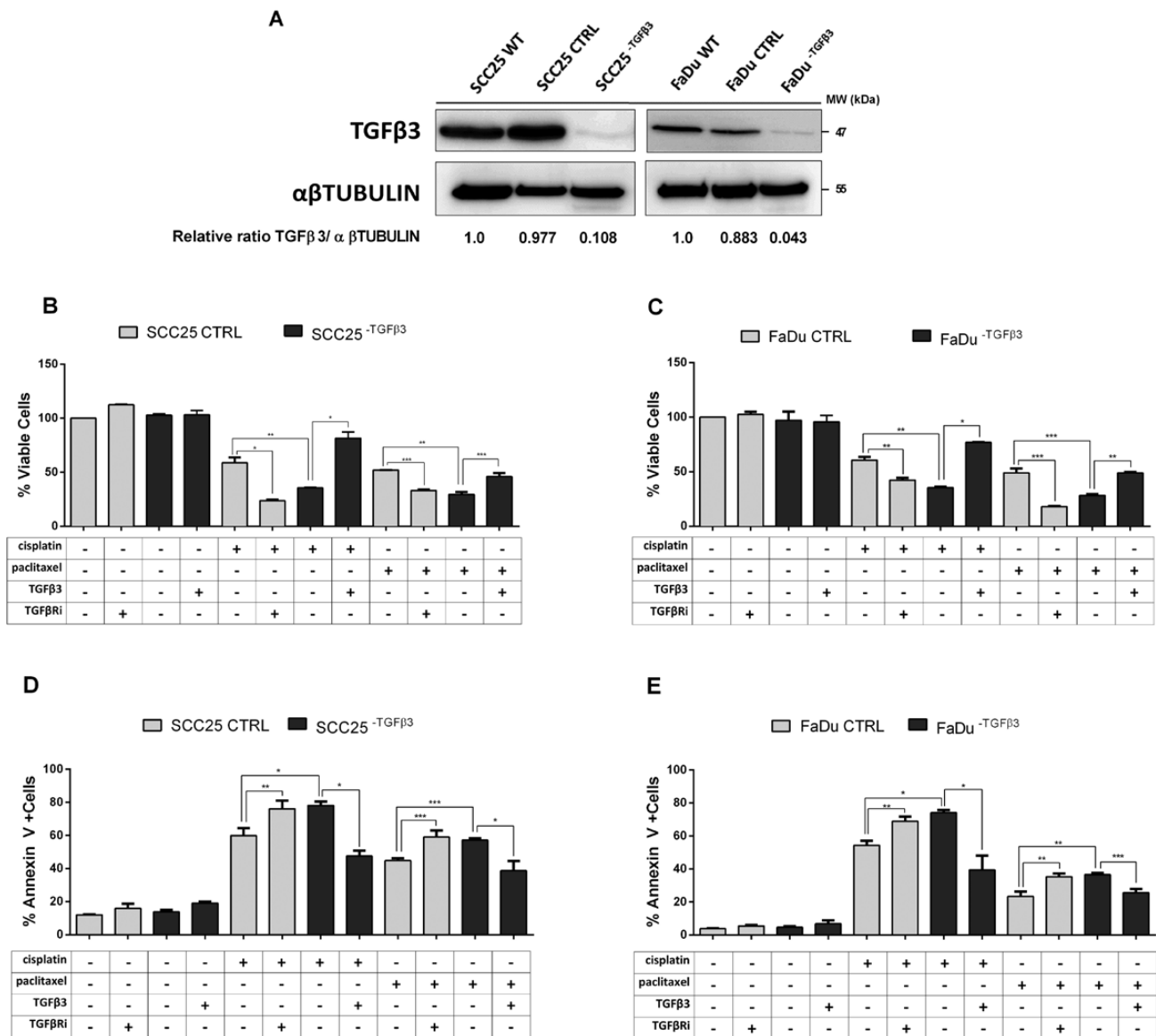


Figure 3. The lack of TGFβ3 sensitizes HNSCC cell lines to cytotoxic therapies. (A) The TGFβ3 knockout was performed with CRISPR-Cas9 system and verified by WB. Knockout of TGFβ3 in SCC25 (B and D) and FaDu (C and E) induces sensitivity to cisplatin and paclitaxel, whereas exogenous TGFβ3 abrogated this sensitivity. The treatment with the inhibitor of TGFβ receptor (TGFβRI) sensitized CTRL HNSCC cells to cisplatin and paclitaxel treatments. HNSCC cell viability was quantified using CellTiter-Glo method (B and C) and apoptosis was assayed by Annexin V staining (D and E). Asterisks denote significance as determined by one-way ANOVA multiple comparisons followed by Bonferroni test (post-test); * $P < 0.0001$, ** $P < 0.01$, *** $P < 0.05$. TGFβ, transforming growth factor beta.

have a high specific binding affinity for ganglioside GM1 or phosphatidylserine present in the membrane of the respective EV fractions. This technique provides a highly specific method for the isolation of phospholipid membrane vesicles with minimal contamination of large non-vesicular biologic complexes or high abundant plasma proteins. Importantly, this method has been used to capture EVs from relatively small volumes of frozen biological fluids such as plasma and ascites to identify biomarkers in preeclampsia and ovarian cancer (30,39).

The importance of these findings is underscored by its clinical relevance. We were able to show, in the context of a controlled clinical trial, that TGFβ3 in plasma AV-EV fraction served as biomarker for CRT response using a readily available ELISA kit. Our data suggest that in this specific set of patients with advanced HNSCC treated with organ-preservation protocol, high TGFβ3 levels in plasma AV-EVs were associated with disease

progression, and with a dose-dependent likelihood of treatment failure on logistic regression models. Although this is a relatively small cohort of 38 patients, the uniformity of within the confines of a phase 2 study contributes to the accuracy of these results and supports the need for a future clinical trial where patients with high levels of TGFβ3 in AV-EVs are directed to more aggressive therapy or curative surgery rather than routine cisplatin-based CRT regimens.

TGFβ pathway has been shown to be important for epithelial mesenchymal transition, stem cell states and treatment resistance (40–42). Previous studies have implicated this pathway in chemoresistance, specifically through TGFβ1 signaling via TGFβRII. In breast cancer, autocrine TGFβ signaling was shown to mediate paclitaxel resistance promoting cell survival via inhibition of apoptotic signaling (41). Furthermore, Oshimori et al. (42) observed that stem cells derived from squamous cell cancer

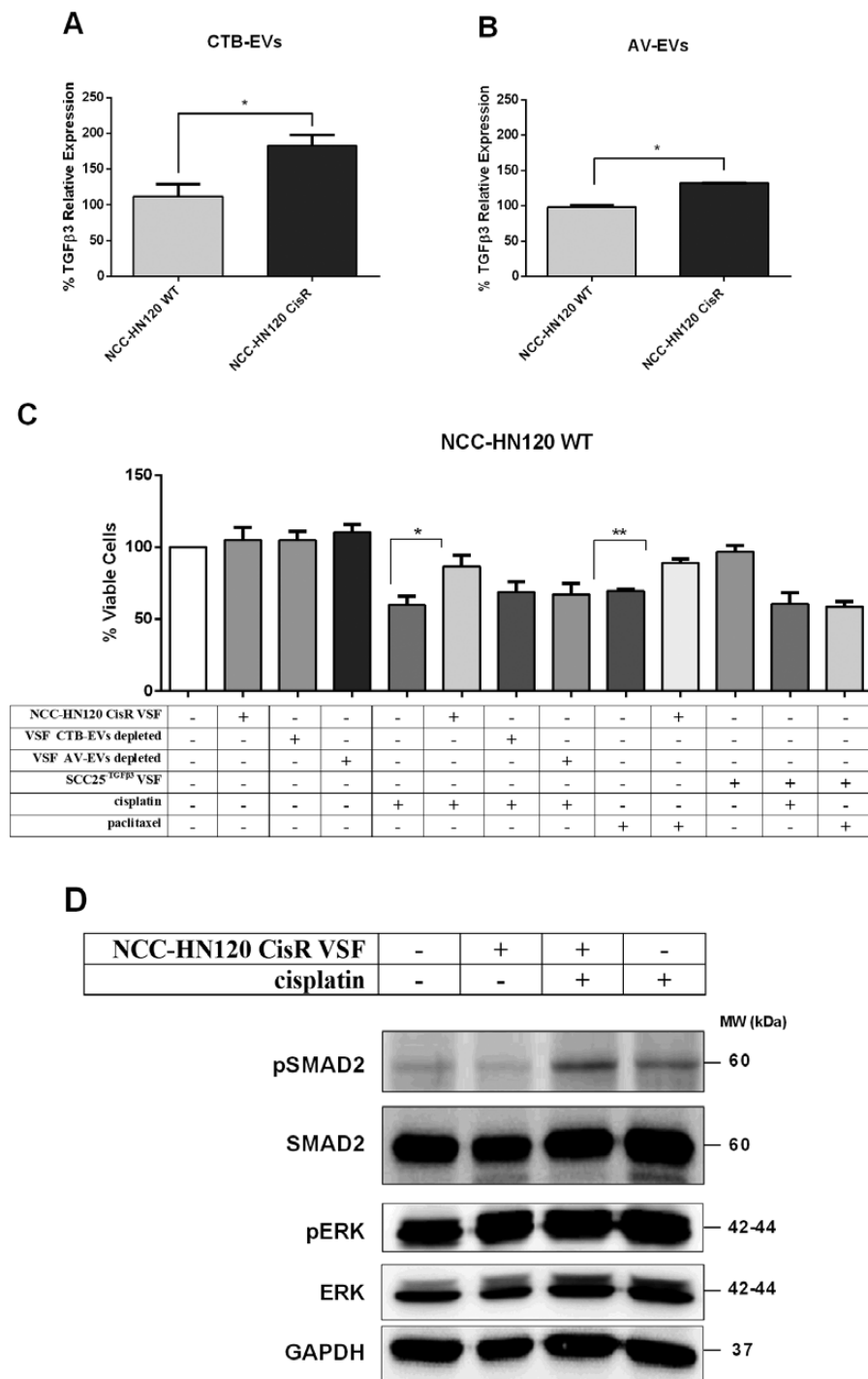


Figure 4. TGF β 3 present in the EVs secreted by CisR HNSCC cells promotes resistance to cisplatin. The relative TGF β 3 expression in CTB-EVs (A) and AV-EVs (B) shed by NCC-HN120 cell lines was measured through ELISA-sandwich (LS-Bio) and normalized by CD81 expression in the EVs. The significance was determined by Student's t-test (two-tailed; * $P = 0.0055$ and * $P = 0.0316$, respectively). (C) NCC-HN120 WT cells were treated with VSF from NCC-HN120 CisR and SCC25^{TGF β 3} on the presence of cisplatin or paclitaxel. Asterisks denote significance as determined by one-way ANOVA, multiple comparisons followed by Bonferroni test (post-test; * $P < 0.0001$ and ** $P = 0.0012$). (D) WB assay showing activation of TGF β pathway after co-treatment of NCC-HN120 WT with VSF from NCC-HN120 CisR cells and cisplatin. GAPDH was used as loading control. AV, Annexin V; CTB, *Cholerae* Toxin chain B; EV, extracellular vesicle; TGF β , transforming growth factor beta; VSF, vesicular secretome fraction.

respond to TGF β 1 treatment with increasing cisplatin resistance. In the latter context, TGF β signaling results in the induction of p21, stabilization of NRF2, thereby markedly enhancing glutathione metabolism and diminishing the effectiveness of anticancer therapy. Several studies have demonstrated that

TGF β signaling is either dependent or independent of SMAD activation, where the major pathways are context dependent or cell-type specific (43). Moreover, Zhu et al. (44) demonstrated that chemotherapeutic agents (cisplatin and paclitaxel) could activate the TGF β pathway by stimulating the phosphorylation

of SMAD2 and SMAD3 in cervical and ovarian cancer cell lines. As such, there is much interest in the role of TGF β inhibitors as potential antimetastatic agents or enhancers of cytotoxic treatment.

In this study, using commercially available lines and isogenic pairs of CisR/sensitive patient-derived lines, we also observed that TGF β pathway plays a major role in HNSCC drug resistance. Specifically, TGF β 3 as being differentially expressed in drug-resistant HNSCC cell lines. Exogenous TGF β 3 induced resistance in drug-sensitive cell lines, whereas LY2109761 (a neutralizing TGF β R2 antibody) sensitized drug-resistant cell lines. Incidentally, LY2109761 has been shown to sensitize a wide range of cancer cell lines (e.g. ovarian cancer, osteosarcoma) to cisplatin (45,46). We also found that HNSCC cell lines secrete TGF β 3 in EV, and the level of this protein in EVs was correlated with drug resistance. EV-enriched VSF from resistant cells conferred resistance when applied to sensitive cells. The depletion of CTB-/AV-EVs reduced the potency of VSF in conferring resistance. In addition, EV-enriched VSF from TGF β 3 knockout cell line could not induce resistance on sensitive cells. VSF-mediated induction of drug resistance resulted in TGF β 3 downstream signaling in sensitive recipient cells with SMAD2 phosphorylation. TGF β 3 in the EVs were significantly higher than matched controls (plasma or cell culture medium), indicating that they are not non-specific contaminants. However, determining the location of TGF β 3 as being membrane-bound or within the lipid-bilayer of the EVs would be important in elucidating the molecular mechanism of action.

The role of EVs in transferring drug resistance is well documented by several mechanisms (11). EV-associated factors mediating drug resistance include DNMT1, miR-214 and miR-21-3p in ovarian cancer; lncRNA-ROR in hepatocellular carcinoma; miR-34a in prostate cancer; miR-100-5p in lung cancer; and miR-21 in gastric cancer cells and in HNSCC (47–53). Other studies have also demonstrated that cancer-cell derived EVs can induce TGF β signaling via TGF β /SMAD pathway activation and enhancing DNA repair activity through SMAD and downstream Lig4 expression, resulting the protection of epithelial cells from γ -radiation stress (54,55). Protein content profiling of EVs shed by 60 cell lines from the National Cancer Institute (NCI-60) found TGF β 3 secreted by melanoma, brain, breast, colon, kidney, lung and ovarian cancers, but not HNSCC (56).

In summary, our results indicate that TGF β 3 transmitted through EVs plays a significant role in HNSCC resistance to cytotoxic therapy. High levels of this protein in plasma EVs is an independent predictor of disease progression in patients with locally advanced HNSCC treated with the chemoradiotherapy. We posit that the use of TGF β R inhibitors could be a novel sensitization approach in HNSCC patients with high TGF β otherwise predicted to fail concurrent CRT. Importantly, these results demonstrate the potential of translating biological hypotheses involving EVs into *bona fide*, clinically relevant biomarkers, using non-invasive monitoring.

Ethical approval

Ethics approval and consent to participate

Written informed consent was obtained from all HNSCC patients. This study was approved by the institution ethics committees (CEP-UNIFESP: 1610/2016; CEP-HCBarretos: 231/2009).

Data availability

The datasets used and/or analyzed during the current study are available from the corresponding author on reasonable request.

Supplementary material

Supplementary data are available at *Carcinogenesis* online.

Funding

This study was supported by grants from National Cancer Centre of Singapore Research Foundation Fundação de Amparo à Pesquisa do Estado de São Paulo—FAPESP (FAPESP, 2015/09182-0) and Exploit Technologies Pte and Biomedical Research Council (A*STAR; ETPL/12-R15GAP-0010). The sponsors had no role in the study design, collection and analysis, interpretation of the data, decision to publish, or writing the manuscript.

Acknowledgements

D.M.R.-Jr acknowledges the support of the Coordenação de Aperfeiçoamento de Pessoal de Nível Superior (CAPES, 99999.007922/2014-00) and of the São Paulo Research Foundation (FAPESP, 2015/21420-3). A.L.V. and A.L.C. had a Conselho Nacional de Desenvolvimento Científico e Tecnológico (CNPq) scholarship (300936/2015-0 and 561217/2010–6, respectively). N.G.I. acknowledges the National Medical Research Council of Singapore Clinician Scientist Award (NMRC/CSA-INV/011/2016).

Conflict of Interest Statement: None declared.

References

- Jemal, A. et al. (2011) Global cancer statistics. *CA. Cancer J. Clin.*, 61, 69–90.
- Ferlay, J. et al. (2013) Cancer incidence and mortality patterns in Europe: estimates for 40 countries in 2012. *Eur. J. Cancer*, 49, 1374–1403.
- Iyer, N.G. et al. (2015) Randomized trial comparing surgery and adjuvant radiotherapy versus concurrent chemoradiotherapy in patients with advanced, nonmetastatic squamous cell carcinoma of the head and neck: 10-year update and subset analysis. *Cancer*, 121, 1599–1607.
- Viana, L.S. et al. (2016) Efficacy and safety of a cisplatin and paclitaxel induction regimen followed by chemoradiotherapy for patients with locally advanced head and neck squamous cell carcinoma. *Head Neck*, 38, e970–e980.
- Lococo, F. et al. (2015) Preliminary evidence on the diagnostic and molecular role of circulating soluble EGFR in non-small cell lung cancer. *Int. J. Mol. Sci.*, 16, 19612–19630.
- Yáñez-Mó, M. et al. (2015) Biological properties of extracellular vesicles and their physiological functions. *J. Extracell. Vesicles*, 4, 27066.
- Colombo, M. et al. (2014) Biogenesis, secretion, and intercellular interactions of exosomes and other extracellular vesicles. *Annu. Rev. Cell Dev. Biol.*, 30, 255–289.
- Tkach, M. et al. (2016) Communication by extracellular vesicles: where we are and where we need to go. *Cell*, 164, 1226–1232.
- Principe, S. et al. (2013) Tumor-derived exosomes and microvesicles in head and neck cancer: implications for tumor biology and biomarker discovery. *Proteomics*, 13, 1608–1623.
- Plebanek, M.P. et al. (2017) Pre-metastatic cancer exosomes induce immune surveillance by patrolling monocytes at the metastatic niche. *Nat. Commun.*, 8, 1319.
- Samuel, P. et al. (2017) Mechanisms of drug resistance in cancer: the role of extracellular vesicles. *Proteomics*, 17, 1600375.
- Gao, L. et al. (2018) Tumor-derived exosomes antagonize innate antiviral immunity. *Nat. Immunol.*, 19, 233–245.
- Ramirez, M.I. et al. (2018) Technical challenges of working with extracellular vesicles. *Nanoscale*, 10, 881–906.
- Ludwig, S. et al. (2017) Suppression of lymphocyte functions by plasma exosomes correlates with disease activity in patients with head and neck cancer. *Clin. Cancer Res.*, 23, 4843–4854.
- Whiteside, T.L. (2016) Exosomes and tumor-mediated immune suppression. *J. Clin. Invest.*, 126, 1216–1223.
- Rodrigues-Junior, D.M. et al. (2019) A preliminary investigation of circulating extracellular vesicles and biomarker discovery associated with

- treatment response in head and neck squamous cell carcinoma. *BMC Cancer*, 19, 373.
17. Cui, W. et al. (1996) TGFbeta1 inhibits the formation of benign skin tumors, but enhances progression to invasive spindle carcinomas in transgenic mice. *Cell*, 86, 531–542.
 18. Lu, S.L. et al. (2006) Loss of transforming growth factor-beta type II receptor promotes metastatic head-and-neck squamous cell carcinoma. *Genes Dev.*, 20, 1331–1342.
 19. Bornstein, S. et al. (2009) Smad4 loss in mice causes spontaneous head and neck cancer with increased genomic instability and inflammation. *J. Clin. Invest.*, 119, 3408–3419.
 20. Lu, S.L. et al. (2004) Overexpression of transforming growth factor beta1 in head and neck epithelia results in inflammation, angiogenesis, and epithelial hyperproliferation. *Cancer Res.*, 64, 4405–4410.
 21. Feltl, D. et al. (2005) The dynamics of plasma transforming growth factor beta 1 (TGF-beta1) level during radiotherapy with or without simultaneous chemotherapy in advanced head and neck cancer. *Oral Oncol.*, 41, 208–213.
 22. Wunderlich, H. et al. (1998) Increased transforming growth factor beta1 plasma level in patients with renal cell carcinoma: a tumor-specific marker? *Urol. Int.*, 60, 205–207.
 23. Kong, F. et al. (1999) Plasma transforming growth factor-beta1 level before radiotherapy correlates with long term outcome of patients with lung carcinoma. *Cancer*, 86, 1712–1719.
 24. Maehara, Y. et al. (1999) Role of transforming growth factor-beta 1 in invasion and metastasis in gastric carcinoma. *J. Clin. Oncol.*, 17, 607–614.
 25. Tsushima, H. et al. (2001) Circulating transforming growth factor beta 1 as a predictor of liver metastasis after resection in colorectal cancer. *Clin. Cancer Res.*, 7, 1258–1262.
 26. Song, B.C. et al. (2002) Transforming growth factor-beta1 as a useful serologic marker of small hepatocellular carcinoma. *Cancer*, 94, 175–180.
 27. Ivanović, V. et al. (2006) Elevated plasma TGF-beta1 levels correlate with decreased survival of metastatic breast cancer patients. *Clin. Chim. Acta.*, 371, 191–193.
 28. Chia, S. et al. (2017) Phenotype-driven precision oncology as a guide for clinical decisions one patient at a time. *Nat. Commun.*, 8, 435.
 29. Rasheed, S.A.K. et al. (2018) GNA13 expression promotes drug resistance and tumor-initiating phenotypes in squamous cell cancers. *Oncogene*, 37, 1340–1353.
 30. Tan, K.H. et al. (2014) Plasma biomarker discovery in preeclampsia using a novel differential isolation technology for circulating extracellular vesicles. *Am. J. Obstet. Gynecol.*, 211, 380e1–3813.
 31. Lai, R.C. et al. (2016) MSC secretes at least 3 EV types each with a unique permutation of membrane lipid, protein and RNA. *J. Extracell. Vesicles*, 5, 29828.
 32. Rodrigues-Junior, D.M. et al. (2018) OIP5 expression sensitize glioblastoma cells to lomustine treatment. *J. Mol. Neurosci.*, 66, 383–389.
 33. Kapral, M. et al. (2008) Transforming growth factor beta isoforms (TGF-beta1, TGF-beta2, TGF-beta3) messenger RNA expression in laryngeal cancer. *Am. J. Otolaryngol.*, 29, 233–237.
 34. Ran, F.A. et al. (2013) Genome engineering using the CRISPR-Cas9 system. *Nat. Protoc.*, 8, 2281–2308.
 35. Arantes, L.M. et al. (2017) MiR-21 as prognostic biomarker in head and neck squamous cell carcinoma patients undergoing an organ preservation protocol. *Oncotarget*, 8, 9911–9921.
 36. Ong, C.J. et al. (2017) A three gene immunohistochemical panel serves as an adjunct to clinical staging of patients with head and neck cancer. *Oncotarget*, 8, 79556–79566.
 37. Wang, W. et al. (2015) An eleven gene molecular signature for extracapsular spread in oral squamous cell carcinoma serves as a prognosticator of outcome in patients without nodal metastases. *Oral Oncol.*, 51, 355–362.
 38. Shao, H. et al. (2012) Protein typing of circulating microvesicles allows real-time monitoring of glioblastoma therapy. *Nat. Med.*, 18, 1835–1840.
 39. Reiner, A.T. et al. (2017) EV-associated MMP9 in high-grade serous ovarian cancer is preferentially localized to annexin V-binding EVs. *Dis. Markers*, 2017, 9653194.
 40. Heldin, C.H. et al. (2009) Mechanism of TGF-beta signaling to growth arrest, apoptosis, and epithelial-mesenchymal transition. *Curr. Opin. Cell Biol.*, 21, 166–176.
 41. Bholra, N.E. et al. (2013) TGF-beta inhibition enhances chemotherapy action against triple-negative breast cancer. *J. Clin. Invest.*, 123, 1348–1358.
 42. Oshimori, N. et al. (2015) TGF-beta promotes heterogeneity and drug resistance in squamous cell carcinoma. *Cell*, 160, 963–976.
 43. Zhang, Y.E. (2009) Non-Smad pathways in TGF-beta signaling. *Cell Res.*, 19, 128–139.
 44. Zhu, H. et al. (2018) A novel TGFbeta trap blocks chemotherapeutics-induced TGFbeta1 signaling and enhances their anticancer activity in gynecologic cancers. *Clin. Cancer Res.*, 24, 2780–2793.
 45. Ren, X.F. et al. (2015) LY2109761 inhibits metastasis and enhances chemosensitivity in osteosarcoma MG-63 cells. *Eur. Rev. Med. Pharmacol. Sci.*, 19, 1182–1190.
 46. Gao, Y. et al. (2015) LY2109761 enhances cisplatin antitumor activity in ovarian cancer cells. *Int. J. Clin. Exp. Pathol.*, 8, 4923–4932.
 47. Corcoran, C. et al. (2014) miR-34a is an intracellular and exosomal predictive biomarker for response to docetaxel with clinical relevance to prostate cancer progression. *Prostate*, 74, 1320–1334.
 48. Takahashi, K. et al. (2014) Extracellular vesicle-mediated transfer of long non-coding RNA ROR modulates chemosensitivity in human hepatocellular cancer. *FEBS Open Bio.*, 4, 458–467.
 49. Pink, R.C. et al. (2015) The passenger strand, miR-21-3p, plays a role in mediating cisplatin resistance in ovarian cancer cells. *Gynecol. Oncol.*, 137, 143–151.
 50. Cao, Y.L. et al. (2017) Exosomal DNMT1 mediates cisplatin resistance in ovarian cancer. *Cell Biochem. Funct.*, 35, 296–303.
 51. Liu, T. et al. (2017) Exosomes containing miR-21 transfer the characteristic of cisplatin resistance by targeting PTEN and PDCD4 in oral squamous cell carcinoma. *Acta. Biochim. Biophys. Sin. (Shanghai)*, 49, 808–816.
 52. Qin, X. et al. (2017) Cisplatin-resistant lung cancer cell-derived exosomes increase cisplatin resistance of recipient cells in exosomal miR-100-5p-dependent manner. *Int. J. Nanomedicine*, 12, 3721–3733.
 53. Zhang, J. et al. (2017) Curcumin suppresses cisplatin resistance development partly via modulating extracellular vesicle-mediated transfer of MEG3 and miR-214 in ovarian cancer. *Cancer Chemother. Pharmacol.*, 79, 479–487.
 54. Gu, J. et al. (2012) Gastric cancer exosomes trigger differentiation of umbilical cord derived mesenchymal stem cells to carcinoma-associated fibroblasts through TGF-beta/Smad pathway. *PLoS One*, 7, e52465.
 55. Lee, J. et al. (2016) TGF-beta1 accelerates the DNA damage response in epithelial cells via Smad signaling. *Biochem. Biophys. Res. Commun.*, 476, 420–425.
 56. Hurwitz, S.N. et al. (2016) Proteomic profiling of NCI-60 extracellular vesicles uncovers common protein cargo and cancer type-specific biomarkers. *Oncotarget*, 7, 86999–87015.